A Theoretical and Experimental Overview of Accelerator RF Systems

Dahee Jang, ID: 20252087, Div. of Advanced Nuclear Engineering, POSTECH, Pohang, Republic of Korea

Abstract

This report presents a comprehensive overview of the theoretical foundations and experimental characterization of radiofrequency (RF) systems employed in particle accelerators. It addresses key RF concepts such as cavity resonance, impedance matching, and wave propagation in transmission lines. Through practical measurements using vector network analyzers (VNAs), time-domain reflectometry (TDR), and stripline beam position monitors (BPM), the report also highlights diagnostic techniques essential for understanding RF behavior. Lastly, it discusses the operational aspects of accelerator subsystems observed during hands-on sessions.

1. Introduction

Radiofrequency (RF) systems are fundamental components of modern accelerators, enabling high-efficiency particle acceleration through time-varying electromagnetic fields. Unlike direct current (DC) systems, RF systems can avoid electrical breakdown by distributing energy via resonant structures. The essential components of these systems include RF sources, transmission lines, resonant cavities, and diagnostics equipment.

Understanding RF operation requires both theoretical analysis and experimental verification. This report outlines the basic theory of RF resonance and impedance, followed by practical experiments aimed at measuring key parameters such as resonance frequency, quality factor, and signal reflection characteristics.

2. RF Cavities and Resonance

RF cavities are designed to support standing electromagnetic waves, providing accelerating fields synchronized with particle bunches. In cylindrical geometries, the modes are classified as TE (transverse electric) and TM (transverse magnetic). For particle acceleration, TM modes are preferred due to their non-zero longitudinal electric field.

The fundamental TM_{010} mode in a pillbox cavity exhibits the following field configuration:

$$
\begin{aligned}
E_z &= E_0 J_0(k_\rho \rho) e^{-i\omega t}, \\
B_\theta &= -i\frac{E_0}{c} J_1(k_\rho \rho) e^{-i\omega t}, \\
k_\rho &= \frac{2.405}{a}, \quad \omega = \frac{2.405c}{a}
\end{aligned}
$$

where a is the cavity radius and J_0, J_1 are Bessel functions of the first kind.

The cavity's performance can be characterized by: - The quality factor $Q = \frac{\omega U}{P_{\text{loss}}}$, indicating energy retention - The shunt impedance $R_s = \frac{V_{\text{acc}}^2}{2P_{\text{loss}}}$, representing RF-to-beam energy conversion efficiency

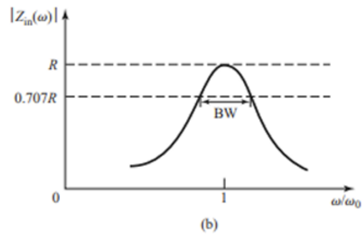

Figure 1: Equivalent RLC circuit model of a resonant RF cavity.

3. Impedance Matching and Smith Chart

In RF systems, impedance mismatches between components cause power reflection and degradation. The voltage reflection coefficient is defined as:

$$\Gamma = \frac{Z_L - Z_0}{Z_L + Z_0}$$

where Z_L is the load impedance and Z_0 the characteristic impedance of the transmission line. Impedance mismatches can be visualized using a Smith chart, which plots complex reflection coefficients and facilitates impedance matching techniques.

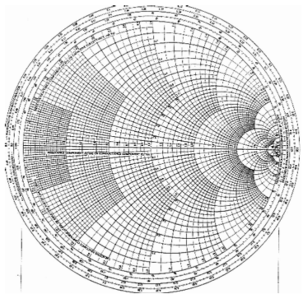

Figure 2: Example of a Smith chart showing impedance trajectory of an RF cavity.

4. Experimental Characterization

4.1 Vector Network Analyzer (VNA)

A VNA measures frequency-dependent S-parameters, which reveal resonance behavior. For a pillbox cavity, S_{11} shows reflection dips at resonant frequencies, and S_{21} exhibits transmission peaks. The quality factor can be extracted from the 3-dB bandwidth.

4.2 Time-Domain Reflectometry (TDR)

TDR sends a step signal down a transmission line and observes reflections caused by impedance mismatches. In the BPM test, reflection spikes were observed at the SMA adapter, suggesting localized mismatches.

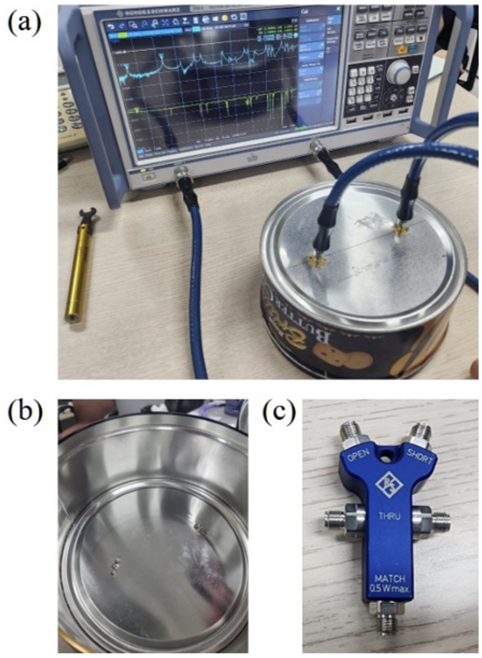

Figure 3: VNA measurement of a pillbox cavity showing S_{11} and S_{21} responses.

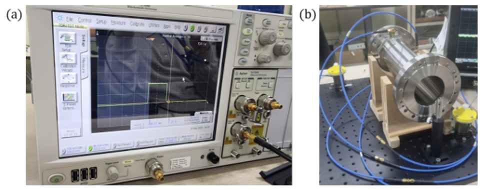

Figure 4: TDR response showing impedance discontinuity at BPM input connector.

4.3 Beam Position Monitor (BPM)

Beam diagnostics were simulated using a 500 MHz sinusoidal signal through a wire placed in the BPM. Four electrodes captured voltage asymmetries, which were used to determine transverse position.

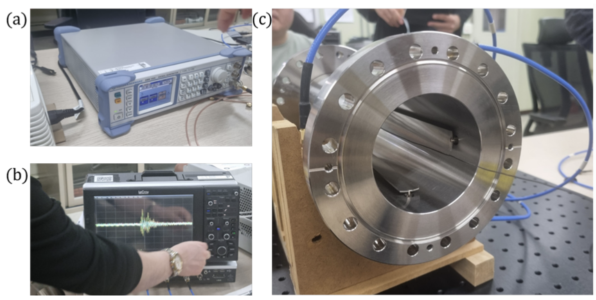

Figure 5: BPM signal acquisition with oscilloscope and signal generator.

5. Accelerator System Overview

The practical aspects of RF systems were explored during a facility tour of an operating linear accelerator. Observations included RF amplifiers, quadrupole magnets, bending sections, and beam dumps. Real-time control software allowed live tuning of RF parameters and beam position monitoring.

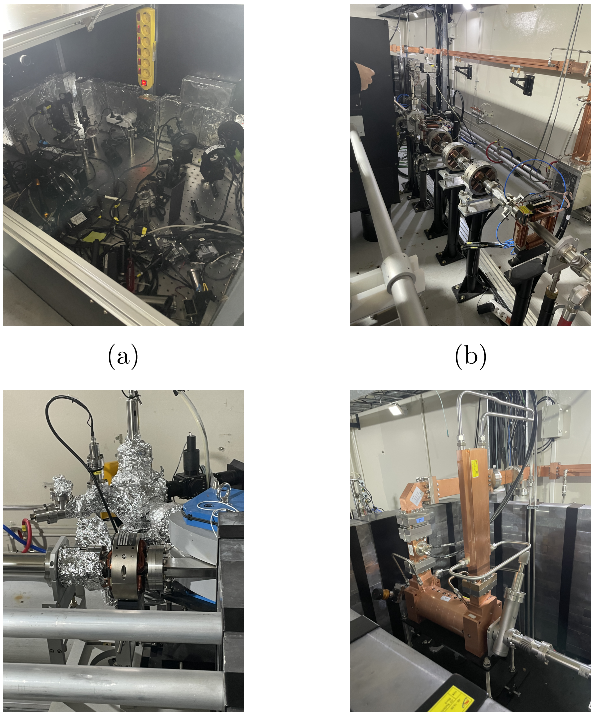

(a) (b) (c) (d)

Figure 6: View of the accelerator subsystem: (a) sample stage, (b) quadrupole magnets surrounding the accelerating tube, (c) bending magnet and diagnostics chamber, and (d) beam dump.

6. Conclusion

This report consolidated theoretical and experimental insights into accelerator RF systems. Key concepts such as cavity resonance and impedance matching were reinforced through measurements using VNA and TDR. The BPM test demonstrated real-world diagnostics capability. A tour of a functioning accelerator further connected theoretical understanding with practical implementation.

References

C. Sung, "Fundamentals of Beam Operation and RF/Beam Diagnostics at eLABs Facility: Part 1," Lecture Notes, NUCE719P-01, Pohang, Republic of Korea, May, 2025.